CAUCHY – Jurnal Matematika Murni dan Aplikasi
Volume 11 (1) (2026), Pages 1033-1048
p-ISSN: 2086-0382; e-ISSN: 2477-3344

Local Stability and Bifurcation Analysis of a Mangrove Detritus Small–Fish Model with Dynamic Harvesting Effort under a Beddington–DeAngelis Functional Response

Donna Kurniasih and Dian Savitri*

Department of Mathematics, Faculty of Mathematics and Natural Sciences, Universitas Negeri Surabaya

Abstract

This study develops a three-dimensional mangrove detritus–small fish model with dynamic harvesting effort governed by a threshold rule and a Beddington–DeAngelis functional response. The objective is to investigate how adaptive harvesting and consumer interference influence the long-term dynamics and local stability of the system. Equilibrium points are derived and analyzed using the Jacobian matrix, eigenvalue-based criteria, numerical simulations, and bifurcation analysis with respect to the threshold parameter. The results show the existence of biologically feasible coexistence equilibria with active harvesting, including stable and unstable branches. A subcritical Hopf bifurcation is detected near $a \approx 6.6159$, indicating a sensitive oscillatory regime in the neighborhood of the coexistence equilibrium. Numerical simulations further show that reduced environmental capacity and increased fish mortality can drive the system toward a no-effort equilibrium in which harvesting collapses. Overall, the threshold parameter acts as a key control factor that can shift the system among stable harvesting, effort extinction, and oscillatory regimes.

Keywords: Beddington–DeAngelis functional response; Hopf bifurcation; dynamic harvesting effort; limit cycle; mangrove ecosystem.

1. Introduction

The mangrove ecosystem ranks among the most productive coastal systems and is crucial for sustaining biological resources and the overall health of the coastal environment. Mangroves provide habitat, serve as nursery grounds, and bolster food webs that sustain diverse groups of flora and fauna with both ecological and economic significance [1]. One key mechanism linking mangrove productivity to consumer communities is the detritus pathway, where mangrove leaf litter decomposes into detritus and becomes an energy source for higher trophic levels [2]. Differences in mangrove species and habitat features may also correlate with variations in associated biota composition within the ecosystem [3]. In addition, mangrove ecosystems support fish populations, including small fish species that utilize mangrove regions [4].

Conversely, mangrove ecosystems are subjected to human-induced pressures that can modify their ecological conditions and functions, such as land conversion and intensive utilization activities. The clearing of land for aquaculture and other forms of exploitation may lead to the

*Corresponding author. E-mail: diansavitri@unesa.ac.id

Submitted: March 09, 2026 Reviewed: April 04, 2026 Accepted: April 20, 2026
DOI: https://doi.org/10.18860/cauchy.v11i1.41486

depletion of mangrove resources and threaten ecosystem sustainability [5]. Small-scale fisheries in mangrove areas can also alter fish community composition and the abundance of particular groups [4]. More generally, harvesting pressure and its consequences for fish stocks remain critical issues in aquatic ecosystem management [6].

Biomathematical modeling offers a quantitative approach for elucidating interactions among ecosystem components and the effects of disturbances on long-term system dynamics. Prey–predator and food–chain models have been employed to investigate system responses to management strategies, such as implementing protection zones that can influence exploitation rates and population trends [7]. Predator–prey models incorporating harvesting are also frequently used to analyze equilibrium existence and local stability [8]. In the fisheries context, predator–prey-based fishery models can exhibit complex dynamics and regime shifts driven by changes in parameters, interaction structures, and harvesting effort [9, 10]. Moreover, periodic behavior and oscillations in prey–predator systems are commonly observed and are important for stability studies and long-term predictions [11].

A crucial aspect of prey–predator modeling is the choice of functional response. Although linear predation terms are often used due to their simplicity, they may be unrealistic when consumption saturates at high resource availability or when predator interference occurs at high predator densities. The Beddington–DeAngelis functional response explicitly accounts for saturation/handling and predator interference, making it more representative in such situations [12]. Nonlinear functional responses are known to affect coexistence conditions and local stability properties of ecological systems [13]. In various ecological model variants, changes in interaction mechanisms may generate instabilities and qualitative shifts that can be examined using bifurcation frameworks [14]. Even in food-web models, incorporating behavioral mechanisms such as fear effects may further modify system dynamics and stability [15].

Although previous studies have provided important insights into ecological dynamics, their modeling focus differs from the present work. Wang and Dong investigated a food-chain model with a protection zone and emphasized the role of spatial protection mechanisms in species coexistence [7]. Chen analyzed stability and bifurcation in a predator–prey model with Michaelis–Menten type prey harvesting, highlighting the influence of nonlinear harvesting on system dynamics [13]. Song et al. studied Hopf, Turing, and Turing–Hopf bifurcations in a diffusive predator–prey system with a Beddington–DeAngelis functional response, with emphasis on spatiotemporal pattern formation [14]. Ibrahim considered optimal harvesting in a predator–prey fishery model with a critical biomass threshold and marine reserve, focusing on bioeconomic control [16]. Related studies have also considered fishing effort as a dynamic variable and examined threshold-related effort behavior, further emphasizing the importance of adaptive harvesting mechanisms in predator–prey systems [17, 18]. Meanwhile, Luis et al. examined a predator–prey model with prey harvesting from the perspective of numerical implementation using a non-standard finite difference scheme [19]. Other studies have shown that predator–prey fishery systems may exhibit complex dynamics and regime shifts under harvesting effort and additional ecological mechanisms [9, 10]. These studies are relevant and informative, but they do not specifically address the combined effects of a detritus-based mangrove resource, threshold-driven adaptive harvesting effort, and a Beddington–DeAngelis functional response within a single three-dimensional ecological model.

Therefore, the novelty of this study lies in the development and analysis of a three-dimensional mangrove detritus–small fish model that simultaneously incorporates a renewable detritus-based resource pathway, dynamic harvesting effort governed by a threshold rule, and a Beddington–DeAngelis functional response. This combination allows us to examine how consumer interference and adaptive harvesting interact to shape equilibrium structure, local stability, and bifurcation behavior in a mangrove ecosystem context. Based on this framework, the present study aims to derive the biologically feasible equilibria of the system, analyze their local stability properties, and investigate qualitative changes in the dynamics through numerical simulations and bifurcation

analysis with respect to the threshold parameter.

To support the analysis, local stability theory is used to characterize the biologically feasible equilibria, while bifurcation analysis is employed to describe dynamic transitions with respect to the threshold parameter [13]. Hopf bifurcation theory provides a basis for understanding the emergence of oscillatory dynamics in nonlinear ecological models [20], whereas continuation-based analysis helps identify BP, LP, and Hopf points and determine how parameter variation modifies equilibrium stability [14, 21]. Numerical schemes that preserve qualitative properties are also important for verifying analytical predictions through simulation [19].

2. Methods

This section describes the methodological framework used in this study, including the literature review, model formulation, equilibrium analysis, local stability assessment, numerical simulation, and bifurcation analysis conducted to investigate the mangrove detritus–small fish system under dynamic harvesting effort.

2.1. Literature Study

The study begins with a literature review on predator–prey and resource–consumer models applied to coastal and mangrove ecosystems, with particular emphasis on detritus-based food webs and harvesting dynamics. Previous works on functional responses such as linear (Lotka–Volterra) and Holling type II forms are reviewed to understand consumer saturation effects. Additionally, studies employing the Beddington–DeAngelis functional response are examined to capture predator interference, which may arise from competition and crowding among consumers. The reviewed literature provides the theoretical basis for selecting the functional response, defining biological assumptions, and identifying meaningful ranges of model parameters relevant to mangrove detritus and small fish populations.

2.2. Model Construction

Based on the literature review, a three-dimensional ordinary differential equation (ODE) model is developed to describe the interactions within a mangrove ecosystem among detritus density $x(t)$, small fish population $y(t)$, and harvesting effort $E(t)$. The detritus compartment $x(t)$ is conceptualized as a foundational renewable resource representing the steady accumulation of organic leaf litter rather than a self-reproducing biological population. This accumulation process is modeled using a logistic–like growth term $rx(1 - x/k)$, where r denotes the net accumulation rate and k represents the maximum carrying capacity of the detritus pool within the mangrove floor. The consumption of detritus by small fish follows a Beddington–DeAngelis functional response to account for both consumer saturation and mutual interference among predators. Fish growth is driven by the assimilation of detritus, while losses result from natural mortality μ and harvesting mortality $uqEy$. Furthermore, the harvesting effort $E(t)$ is governed by an adaptive threshold rule: it expands when fish density exceeds the profitability threshold a and contracts when it falls below, reflecting the adaptive response of fishers to perceived stock availability.

2.3. Equilibrium points

The equilibrium points of the model are obtained by setting the time derivatives of all state variables equal to zero, i.e., $\dot{x} = \dot{y} = \dot{E} = 0$. Solving the resulting algebraic system yields boundary equilibria (including extinction and fish-free states) as well as coexistence equilibria. Because the effort equation implies $E = 0$ or $y = a$ at equilibrium, two coexistence regimes are possible: a coexistence equilibrium without harvesting ($E = 0$) and a coexistence equilibrium with active harvesting ($E > 0$, hence $y = a$). When explicit closed-form expressions are cumbersome, equilibrium values are characterized implicitly (e.g., as positive roots of algebraic equations) and

subsequently approximated numerically. Only equilibria in the biologically feasible region $x \geq 0$, $y \geq 0$, and $E \geq 0$ are considered for ecological interpretation.

2.4. Local Stability Analysis

Local stability of each equilibrium point is investigated by linearizing the system around the equilibrium using the Jacobian matrix. The symbolic derivation of the Jacobian entries and the subsequent numerical computation of eigenvalues for each equilibrium state are performed using Maple to ensure analytical precision. For boundary equilibria, stability conditions are derived directly from the signs of the eigenvalues. For the coexistence equilibrium with active harvesting, stability is assessed through the Routh–Hurwitz criteria applied to the characteristic polynomial. Furthermore, periodic-orbit continuation is used to investigate the behavior of periodic branches near the Hopf bifurcation point, including the detection of a limit point of cycles (LPC).

2.5. Numerical Simulation

Numerical simulations are performed to support and illustrate the analytical results. The ODE system is solved numerically using MATLAB with the `ode45` solver, employing a relative tolerance of 10^{-6} and an absolute tolerance of 10^{-8} to ensure convergence and accuracy. Simulations are conducted under representative non-negative initial conditions to verify the global attraction of trajectories toward predicted stable states. Several scenarios are considered by varying the threshold parameter a, which directly controls the adaptive harvesting response. Additionally, bifurcation analysis and equilibrium continuation are carried out using MATCONT with an initial step size of 0.01 and a maximum step size of 0.1 to accurately track equilibrium branches and detect critical points such as Hopf (H) and Limit Point (LP) bifurcations.

3. Results and Discussion

This section presents the analytical and numerical results of the three-dimensional mangrove ecosystem model developed to describe the dynamics among detritus, small fish population, and harvesting effort. First, the equilibrium points of the system are identified to describe the possible long-term population and bionomic states. Next, the local stability properties of each equilibrium are analyzed using the Jacobian matrix and the Routh-Hurwitz criterion to determine conditions for system stability. The theoretical findings are then supported by numerical simulations under various parameter scenarios, focusing particularly on the influence of the Beddington–DeAngelis predator interference and the harvesting threshold. Finally, the results are discussed to interpret their ecological implications and to evaluate sustainable harvesting management strategies in mangrove areas.

3.1. Mathematical Model

This predator–prey interaction model was developed to describe the population dynamics within a mangrove ecosystem, specifically focusing on the interaction between leaf litter detritus and small fish. The model incorporates a Beddington–DeAngelis functional response to represent the predation process and accounts for human intervention through bionomic harvesting effort. In this framework, the Beddington–DeAngelis response is used to describe the consumption of detritus by small fish, taking into account both the handling time by the predator and the mutual interference among predators. Furthermore, the harvesting effort is modeled as a dynamic variable that changes based on the density of the fish population relative to an economic or biological threshold. Based on these biological assumptions, the mathematical model can be written as the following system of ordinary differential equations:

$$\begin{aligned}\frac{dx}{dt} &= rx\left(1-\frac{x}{k}\right)-\frac{\alpha xy}{1+cy+bx},\\ \frac{dy}{dt} &= \frac{\beta xy}{1+cy+bx}-\mu y-uqEy,\\ \frac{dE}{dt} &= uqE(y-a).\end{aligned} \tag{1}$$

In the model (1), x, y, and E represent the density of mangrove leaf litter detritus, the population of small fish, and the harvesting effort, respectively. The parameters $r, k, \alpha, c, b, \beta, \mu, u, q$, and a represent the detritus growth rate, environmental carrying capacity, predation rate, predator interference coefficient, handling time, conversion efficiency, natural mortality rate of the fish, economic gain factor, catchability coefficient, and the population threshold for harvesting profitability. Model (1) is given under the initial conditions $x(0) > 0, y(0) > 0$, and $E(0) > 0$, where all parameters are assumed to be positive.

3.2. Positivity and Boundedness of Solutions

Lemma 1. *Suppose $x(0) \geq 0$, $y(0) \geq 0$, and $E(0) \geq 0$. Then the solutions $(x(t), y(t), E(t))$ of system (1) remain nonnegative for all $t \geq 0$.*

Proof. On the boundary planes we have

$$\dot{x}\big|_{x=0} = 0, \qquad \dot{y}\big|_{y=0} = 0, \qquad \dot{E}\big|_{E=0} = 0.$$

Hence, trajectories cannot cross from the nonnegative orthant into the negative region. Therefore, any solution starting in $\mathbb{R}^3_+$ remains in $\mathbb{R}^3_+$ for all $t \geq 0$. □

Lemma 2. *Let $x(0) \geq 0$. Then*

$$0 \leq x(t) \leq \max\{x(0), k\} \qquad \text{for all } t \geq 0.$$

In particular, if $x(0) \leq k$, then $x(t) \leq k$ for all $t \geq 0$.

Proof. Since $\dfrac{\alpha xy}{1+bx+cy} \geq 0$ for $x, y \geq 0$, we obtain

$$\dot{x} = rx\left(1-\frac{x}{k}\right)-\frac{\alpha xy}{1+bx+cy} \leq rx\left(1-\frac{x}{k}\right).$$

By the comparison theorem with the logistic equation, $x(t)$ cannot exceed $\max\{x(0), k\}$ for $t \geq 0$, which proves the claim. □

Lemma 3. *Assume all parameters in system (1) are positive with $\beta > 0$. Then all solutions of the system are uniformly bounded in a compact region $\Omega \subset \mathbb{R}^3_+$.*

Proof. Define the function

$$W(t) = x(t) + \frac{\alpha}{\beta}y(t) + \frac{\alpha}{\beta}E(t).$$

Using system (1) and writing $D = 1 + bx + cy$, we obtain

$$\begin{aligned}\frac{dW}{dt} &= \dot{x} + \frac{\alpha}{\beta}\dot{y} + \frac{\alpha}{\beta}\dot{E} \\ &= rx\left(1 - \frac{x}{k}\right) - \frac{\alpha xy}{D} + \frac{\alpha}{\beta}\left(\frac{\beta xy}{D} - \mu y - uqEy\right) + \frac{\alpha}{\beta}\left(uqE(y-a)\right) \\ &= rx\left(1 - \frac{x}{k}\right) - \frac{\alpha\mu}{\beta}y - \frac{\alpha uqa}{\beta}E.\end{aligned}$$

Let $0 < \eta \leq \min\{\mu, uqa\}$. Then

$$\begin{aligned}\frac{dW}{dt} + \eta W &= rx\left(1 - \frac{x}{k}\right) + \eta x + \frac{\alpha}{\beta}(\eta - \mu)y + \frac{\alpha}{\beta}(\eta - uqa)E \\ &\leq (r + \eta)x - \frac{r}{k}x^2.\end{aligned}$$

The right-hand side attains its maximum at $x = \dfrac{k(r+\eta)}{2r}$, and thus

$$(r + \eta)x - \frac{r}{k}x^2 \leq \frac{k(r+\eta)^2}{4r} =: C.$$

Hence,

$$\frac{dW}{dt} + \eta W \leq C.$$

By the differential inequality theorem, $W(t)$ is uniformly bounded for $t \geq 0$, and consequently

$$x(t) \leq W(t), \qquad y(t) \leq \frac{\beta}{\alpha}W(t), \qquad E(t) \leq \frac{\beta}{\alpha}W(t),$$

which implies that $(x(t), y(t), E(t))$ is uniformly bounded in $\mathbb{R}^3_+$. □

3.3. Equilibrium points

The equilibrium points of system (1) are obtained by setting

$$\dot{x} = 0, \qquad \dot{y} = 0, \qquad \dot{E} = 0. \tag{2}$$

Equivalently, we solve

$$rx\left(1 - \frac{x}{k}\right) - \frac{\alpha xy}{1 + bx + cy} = 0, \tag{3}$$

$$\frac{\beta xy}{1 + bx + cy} - \mu y - uqEy = 0, \tag{4}$$

$$uqE(y - a) = 0. \tag{5}$$

For convenience, define $D = 1 + bx + cy$. From Eq. (5), any equilibrium must satisfy either $E = 0$ (no-harvesting branch) or $y = a$ (active-harvesting branch with $E > 0$). The biologically feasible equilibria are listed below.

1. The trivial equilibrium
$$E_0 = (0, 0, 0),$$
which represents the extinction of detritus, small fish, and harvesting effort.
2. The detritus-only equilibrium
$$E_1 = (k, 0, 0),$$

which represents persistence of detritus at the carrying capacity in the absence of fish and harvesting.

3. The coexistence equilibrium without harvesting effort

$$E_2 = (x_2, y_2, 0),$$

which corresponds to coexistence of detritus and fish when harvesting effort is absent ($E = 0$). For $E = 0$ and $y_2 > 0$, dividing Eq. (4) by y yields

$$\frac{\beta x}{1 + bx + cy} = \mu, \tag{6}$$

so that

$$y_2 = \frac{x_2(\beta - \mu b) - \mu}{\mu c}. \tag{7}$$

Substituting Eq. (7) into Eq. (3) gives an algebraic equation (quadratic) for x_2. The equilibrium E_2 is biologically feasible provided that $x_2 > 0$ and $y_2 > 0$.

4. The coexistence equilibrium with active harvesting

$$E_3 = (x^*, y^*, E^*), \qquad x^* > 0,\ y^* > 0,\ E^* > 0.$$

Since $E^* > 0$, Eq. (5) implies

$$y^* = a. \tag{8}$$

Substituting Eq. (8) into Eq. (3) (and dividing by $x > 0$) yields

$$r\left(1 - \frac{x}{k}\right) = \frac{\alpha a}{1 + bx + ca}, \tag{9}$$

which can be rearranged into a quadratic equation for x^*. Therefore, depending on the parameter values, Eq. (9) may admit *two distinct positive roots* $x_3^{(1)}$ and $x_3^{(2)}$. For each positive root $x_3^{(i)}$ $(i = 1, 2)$, substituting $(x, y) = (x_3^{(i)}, a)$ into Eq. (4) and dividing by $a > 0$ gives

$$E_3^{(i)} = \frac{1}{uq}\left(\frac{\beta x_3^{(i)}}{1 + bx_3^{(i)} + ca} - \mu\right), \qquad i = 1, 2. \tag{10}$$

Hence, the active-harvesting equilibrium may consist of two biologically feasible equilibria

$$E_3^{(1)} = (x_3^{(1)}, a, E_3^{(1)}) \quad \text{and} \quad E_3^{(2)} = (x_3^{(2)}, a, E_3^{(2)}),$$

provided that $x_3^{(i)} > 0$ and $E_3^{(i)} > 0$ for $i = 1, 2$.

> **Remark 1.** The algebraic system (3)–(5) may admit additional solutions with negative components. Such equilibria are mathematically admissible but biologically infeasible, and thus are omitted.

3.4. Local Stability

Local stability of each equilibrium point is investigated by linearizing system (1) around the equilibrium using the Jacobian matrix. For convenience, define

$$D = 1 + bx + cy.$$

Let

$$\dot{x} = f_1(x, y, E), \qquad \dot{y} = f_2(x, y, E), \qquad \dot{E} = f_3(x, y, E),$$

where

$$f_1 = rx\left(1 - \frac{x}{k}\right) - \frac{\alpha xy}{D}, \qquad f_2 = \frac{\beta xy}{D} - \mu y - uqEy, \qquad f_3 = uqE(y - a).$$

The Jacobian matrix is

$$J(x, y, E) = \begin{pmatrix} D_{11} & D_{12} & 0 \\ D_{21} & D_{22} & D_{23} \\ 0 & D_{32} & D_{33} \end{pmatrix}, \tag{11}$$

with entries given by

$$\begin{aligned} D_{11} &= r\left(1 - \frac{2x}{k}\right) - \alpha y\,\frac{D - bx}{D^2}, \\ D_{12} &= -\alpha x\,\frac{D - cy}{D^2}, \\ D_{21} &= \beta y\,\frac{D - bx}{D^2}, \\ D_{22} &= \beta x\,\frac{D - cy}{D^2} - \mu - uqE, \\ D_{23} &= -uqy, \qquad D_{32} = uqE, \qquad D_{33} = uq(y - a). \end{aligned}$$

Theorem 1. *The equilibrium point $E_0 = (0, 0, 0)$ is unstable.*

Proof. Substituting $E_0 = (0, 0, 0)$ into Eq. (11) yields

$$J(E_0) = \begin{pmatrix} r & 0 & 0 \\ 0 & -\mu & 0 \\ 0 & 0 & -uqa \end{pmatrix}.$$

Hence, the eigenvalues are $\lambda_1 = r > 0$, $\lambda_2 = -\mu < 0$, and $\lambda_3 = -uqa < 0$. Since one eigenvalue is positive, E_0 is unstable. □

Theorem 2. *The boundary equilibrium point $E_1 = (k, 0, 0)$ is locally asymptotically stable if*

$$\frac{\beta k}{1 + bk} < \mu,$$

and unstable if $\frac{\beta k}{1+bk} > \mu$.

Proof. Substituting $E_1 = (k, 0, 0)$ into Eq. (11) gives

$$J(E_1) = \begin{pmatrix} -r & -\dfrac{\alpha k}{1 + bk} & 0 \\ 0 & \dfrac{\beta k}{1 + bk} - \mu & 0 \\ 0 & 0 & -uqa \end{pmatrix}.$$

Thus, the eigenvalues are $\lambda_1 = -r < 0$, $\lambda_2 = \frac{\beta k}{1+bk} - \mu$, and $\lambda_3 = -uqa < 0$. Therefore, E_1 is locally asymptotically stable if $\lambda_2 < 0$, i.e. $\frac{\beta k}{1+bk} < \mu$. □

Theorem 3. *Let $E_2 = (x_2, y_2, 0)$ be the coexistence equilibrium without harvesting effort. Then E_2 is locally asymptotically stable if $y_2 < a$, $\mathrm{tr}(J_2) < 0$, and $\det(J_2) > 0$.*

Proof. Evaluating Eq. (11) at $E_2 = (x_2, y_2, 0)$ yields

$$J(E_2) = \begin{pmatrix} D_{11}^{(2)} & D_{12}^{(2)} & 0 \\ D_{21}^{(2)} & D_{22}^{(2)} & -uqy_2 \\ 0 & 0 & uq(y_2 - a) \end{pmatrix},$$

where $D_{ij}^{(2)}$ denotes D_{ij} evaluated at $(x, y, E) = (x_2, y_2, 0)$. This matrix is block triangular, hence one eigenvalue is $\lambda_3 = uq(y_2 - a)$, which is negative if $y_2 < a$. The remaining two eigenvalues are the roots of the characteristic polynomial of the 2×2 block

$$J_2 = \begin{pmatrix} D_{11}^{(2)} & D_{12}^{(2)} \\ D_{21}^{(2)} & D_{22}^{(2)} \end{pmatrix}.$$

For a planar system, both eigenvalues have negative real parts if $\mathrm{tr}(J_2) < 0$ and $\det(J_2) > 0$. Therefore, E_2 is locally asymptotically stable if $y_2 < a$, $\mathrm{tr}(J_2) < 0$, and $\det(J_2) > 0$. □

Theorem 4. *Let $E_3 = (x^*, a, E^*)$ be the coexistence equilibrium with active harvesting ($E^* > 0$). The equilibrium E_3 is locally asymptotically stable if the Routh–Hurwitz conditions*

$$A_1 > 0, \quad A_2 > 0, \quad A_3 > 0, \quad \text{and} \quad A_1 A_2 > A_3$$

hold for the characteristic polynomial of $J(E_3)$.

Proof. Since $E^* > 0$, we have $y^* = a$, and thus $D_{33} = uq(y - a) = 0$ at E_3. Hence,

$$J(E_3) = \begin{pmatrix} D_{11}^* & D_{12}^* & 0 \\ D_{21}^* & D_{22}^* & -uqa \\ 0 & uqE^* & 0 \end{pmatrix},$$

where D_{ij}^* denotes D_{ij} evaluated at $(x, y, E) = (x^*, a, E^*)$. The characteristic polynomial can be written as

$$\lambda^3 + A_1\lambda^2 + A_2\lambda + A_3 = 0,$$

with

$$A_1 = -(D_{11}^* + D_{22}^*), \qquad A_2 = (D_{11}^* D_{22}^* - D_{12}^* D_{21}^*) + u^2 q^2 a E^*, \qquad A_3 = -D_{11}^*\, u^2 q^2 a E^*.$$

By the Routh–Hurwitz criterion for a cubic polynomial, all roots have negative real parts if and only if $A_1 > 0$, $A_2 > 0$, $A_3 > 0$, and $A_1 A_2 > A_3$. This completes the proof. □

3.5. Numerical Simulation

To ensure reproducibility of the numerical simulations, the baseline parameter values used throughout this study are summarized in Table 1. Numerical simulations are carried out to illustrate changes in system dynamics around the equilibrium points. In particular, the evolution of mangrove detritus, small fish, and harvesting effort is visualized through time-series plots and phase portraits.

Table 1: Baseline parameter values used in the numerical simulations

Parameter	Description	Value	Source
r	Intrinsic regeneration rate of detritus	3	Assumed
k	Carrying capacity of detritus	100	Assumed
α	Maximum consumption rate	1.8	[14]
β	Conversion efficiency	0.7	Assumed
μ	Natural mortality rate of fish	0.2	Assumed
q	Catchability coefficient	1	[16]
u	Harvesting intensity factor	1	[16]
b	Saturation parameter	0.3	[14]
c	Interference parameter	0.4	[14]
a	Threshold density for harvesting effort	6	[16]

Parameters without direct literature sources were selected as illustrative values to ensure biologically feasible equilibria and to demonstrate the qualitative dynamical regimes of the model.

For the baseline parameter set in Table 1, the active-harvesting equilibrium was obtained by numerically solving the equilibrium Eqs. (3)–(5) under the condition $y = a$. The Jacobian matrix (11) was then evaluated at the computed equilibrium, and its eigenvalues were calculated numerically using Maple/MATLAB. The resulting biologically feasible active-harvesting equilibrium is

$$E_3 = (x^*, y^*, E^*) = (87.90830066,\ 6,\ 1.866868107),$$

which is locally asymptotically stable. This is confirmed by the eigenvalues of the Jacobian at E_3,

$$\lambda_1 = -2.30467551, \qquad \lambda_{2,3} = -0.08893073 \pm 3.35379932\, i,$$

whose real parts are all negative.

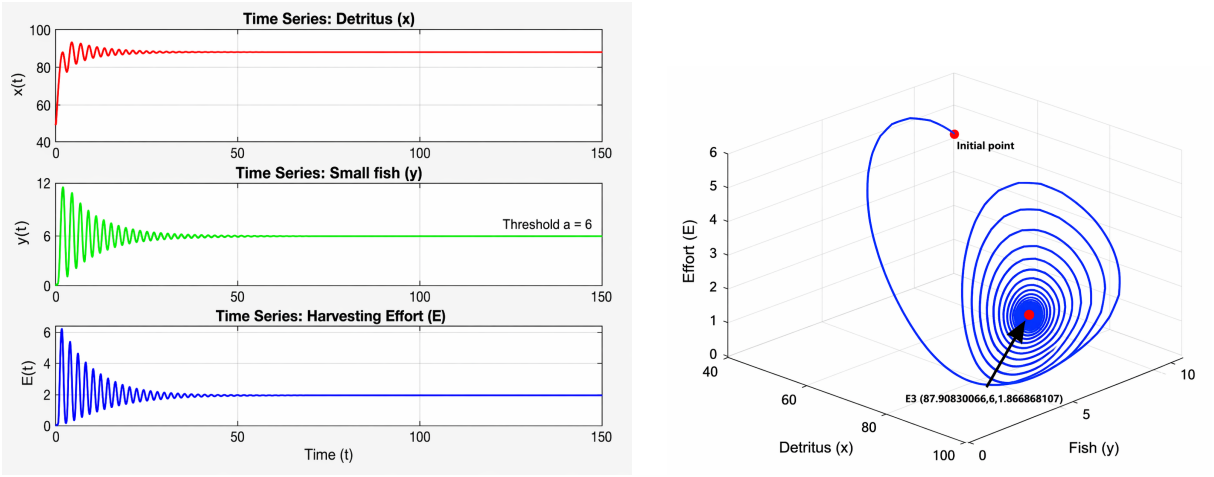

(a) Time series of $x(t)$, $y(t)$, and $E(t)$. **(b)** 3D phase portrait in the (x, y, E)-space.

Fig. 1: Numerical dynamics of system (1) for the baseline parameter set in Table 1, with IC $(x_0, y_0, E_0) = (40, 10, 5)$. The solution exhibits transient oscillations with decreasing amplitudes and converges to the stable equilibrium $E_3 = (87.90830066, 6, 1.866868107)$.

Based on Fig. 1, the trajectories of the detritus density $x(t)$, the small fish density $y(t)$, and the harvesting effort $E(t)$ exhibit transient oscillations with gradually decreasing amplitudes before settling to constant values. This pattern indicates that the solution is attracted to the active-harvesting equilibrium $E_3 = (87.90830066, 6, 1.866868107)$. In particular, the fish density approaches the threshold level $y = a = 6$, while the effort converges to a positive constant, suggesting persistence of harvesting activity in the long term under the chosen parameter set.

The three-dimensional phase portrait in Fig. 1 provides a geometric confirmation of this convergence. Starting from a positive initial condition, the trajectory forms a spiral that contracts toward the equilibrium point E_3. This spiral-in behavior is consistent with the complex conjugate eigenvalues with negative real parts, implying that the system approaches equilibrium through damped oscillations rather than monotone convergence. Biologically, the transient fluctuations reflect short-term adjustments in the detritus–fish interaction and the adaptive response of harvesting effort; however, these fluctuations are eventually regulated, leading to a stable coexistence regime in which detritus, small fish, and a positive harvesting effort persist.

Overall, the time-series plots and the phase portrait consistently demonstrate that, for $a = 6$ and the baseline parameter values in Table 1, system (1) converges to the stable equilibrium E_3, indicating stable coexistence with active harvesting.

To further examine how environmental capacity and fish mortality influence the persistence of harvesting activity, we next consider a second simulation scenario. While the baseline parameter set leads to convergence toward the active-harvesting equilibrium E_3 with positive effort, a reduction in the detritus carrying capacity and an increase in fish natural mortality may suppress harvesting viability. Therefore, we modify only two parameters, namely the carrying capacity $k = 10$ and the fish mortality rate $\mu = 0.6$, and investigate whether the system transitions to a no-effort equilibrium where harvesting effort vanishes. For the modified parameter set $(k, \mu) = (10, 0.6)$, the no-effort equilibrium was obtained by solving Eqs. (3)–(5) with $E = 0$, and its stability was checked from the Jacobian eigenvalues. The resulting biologically feasible equilibrium is

$$E_2 = (x_2, y_2, 0) = (3.059504293,\ 4.128925969,\ 0).$$

The Jacobian matrix evaluated at this equilibrium has eigenvalues

$$\lambda_{1,2} = -0.33003072 \pm 0.70419535\, i, \qquad \lambda_3 = -1.87107403,$$

whose real parts are all negative. Hence, E_2 is locally asymptotically stable.

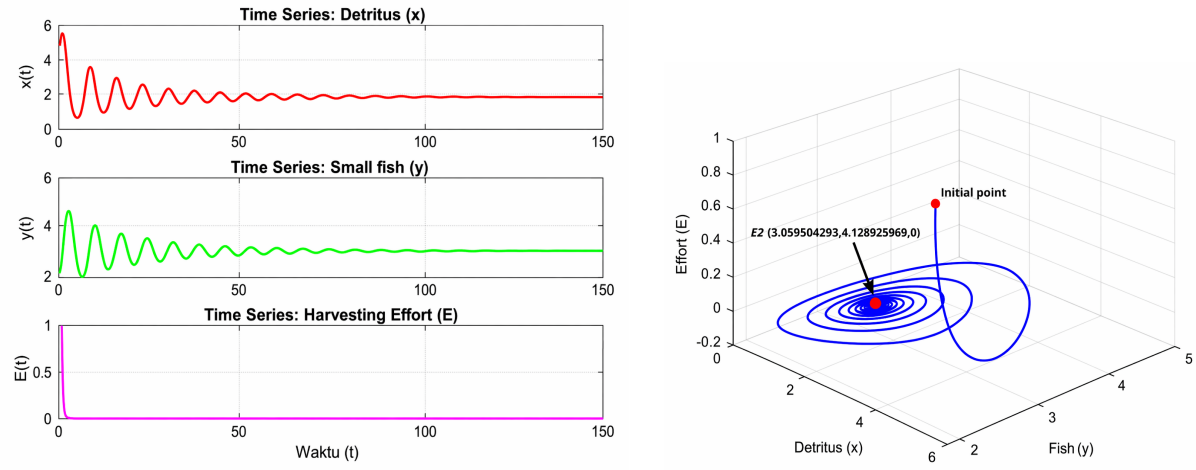

(a) Time series of $x(t)$, $y(t)$, and $E(t)$. **(b)** 3D phase portrait in the (x, y, E)-space.

Fig. 2: Numerical dynamics of system (1) under the modified parameters $k = 10$ and $\mu = 0.6$ (other parameters fixed), with IC $(x_0, y_0, E_0) = (5, 2, 1)$. The trajectory converges to the no-effort equilibrium $E_2 = (3.059504293,\ 4.128925969,\ 0)$.

Fig. 2(a) shows that the detritus density $x(t)$ and the fish density $y(t)$ undergo damped oscillations and eventually approach constant values. In contrast, the harvesting effort quickly decreases to $E(t) \approx 0$ and remains at zero thereafter. This indicates that the system is attracted to the no-effort coexistence equilibrium $E_2 = (3.059504293,\ 4.128925969,\ 0)$, where detritus and fish persist but harvesting activity collapses.

The convergence is further illustrated by the three-dimensional phase portrait in Fig. 2(b). Starting from a positive initial condition, the trajectory spirals toward the equilibrium point lying on the plane $E = 0$. Biologically, decreasing the carrying capacity k limits detritus availability, while increasing the mortality rate μ reduces fish persistence; together, these effects weaken the stock-effort feedback and drive the adaptive harvesting effort toward extinction. In the second scenario, where environmental capacity is reduced ($k = 10$) and mortality is increased ($\mu = 0.6$), the system converges to the no-effort equilibrium $E_2 \approx (3.06, 4.13, 0)$. For this equilibrium, the relation

$$\frac{\beta x_2}{1 + bx_2 + cy_2} = \mu$$

holds from the equilibrium equation with $E = 0$, while local stability is verified by the conditions in Theorem 3.5 and confirmed numerically by the Jacobian eigenvalues, whose real parts are all negative. This confirms that reduced detritus availability and higher fish mortality can render active harvesting unviable, leading to the collapse of fishing effort. Hence, compared with the baseline case leading to a stable positive-effort equilibrium E_3, the modified scenario demonstrates that changes in environmental capacity and mortality can shift the system to a stable regime without harvesting.

Overall, the two simulation scenarios indicate that the model may switch between an active-harvesting steady state (E_3) and a no-effort regime (E_2) depending on environmental capacity and fish mortality.

3.6. Bifurcation with respect to the threshold parameter a

This subsection investigates qualitative changes in the system dynamics when the threshold parameter a is treated as the bifurcation parameter. Numerical continuation is performed using MATCONT to trace equilibrium branches and detect critical bifurcation points associated with changes in local stability and long-term behavior.

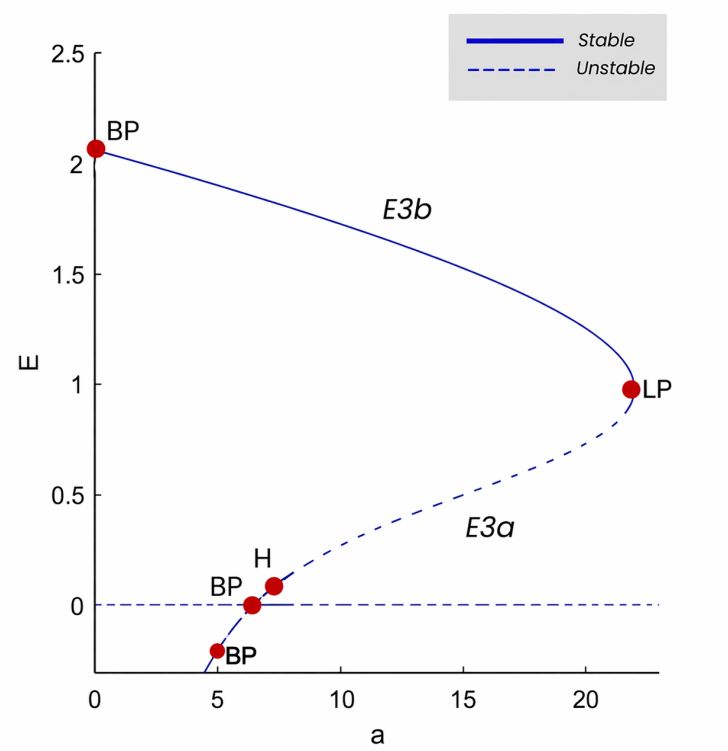

Fig. 3: Bifurcation diagram in the (a, E)-plane obtained by MATCONT. Solid and dashed curves represent stable and unstable equilibrium segments, respectively. Detected singular points include branch points (BP), a Hopf bifurcation (H), and a limit point (LP).

Fig. 3 shows the equilibrium continuation results in the (a, E)-plane. Two branches of biologically feasible active-harvesting equilibria are observed, denoted by E_{3b} and E_{3a}. The branch E_{3b} is stable, while E_{3a} is unstable. The existence of these two branches indicates that, for certain ranges of the threshold parameter, the model admits multiple coexistence equilibria with positive harvesting effort.

A fold bifurcation is detected at the limit point (LP), located at approximately

$$(x, y, E, a) \approx (33.666010,\ 22.000996,\ 0.984220,\ 22.000996).$$

This point marks a turning point of the equilibrium branch and indicates a parameter threshold at which the number of biologically feasible equilibria may change. In addition, branch points (BP) are detected near the boundary branch $E \approx 0$, including a biologically relevant BP at

$$(x, y, E, a) \approx (1.120070,\ 6.460557,\ 0,\ 6.460557),$$

suggesting a structural change of the equilibrium branch near the no-effort regime. A Hopf bifurcation is detected on the lower branch at approximately

$$(x, y, E, a) \approx (1.243956,\ 6.615926,\ 0.016633,\ 6.615926).$$

Moreover, MATCONT computes the first Lyapunov coefficient

$$l_1 \approx 6.337488 \times 10^{-2} > 0,$$

which indicates that the Hopf bifurcation is subcritical. Hence, the transition near the Hopf point should be interpreted as a sensitive local change in dynamics. Solutions with negative effort are mathematically admissible but biologically infeasible and are therefore excluded from ecological interpretation.

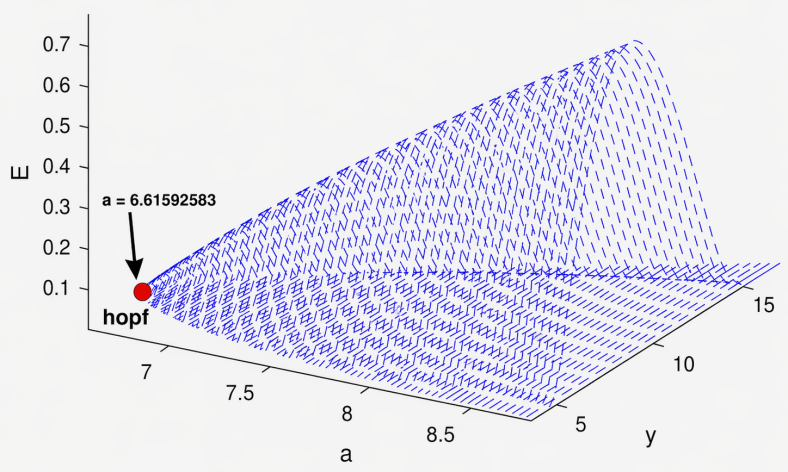

Fig. 4: Periodic-orbit continuation near the Hopf bifurcation point ($a \approx 6.61592583$), showing an unstable periodic branch near the subcritical Hopf point and a change in stability along the branch through a limit point of cycles (LPC).

Fig. 4 provides numerical evidence of periodic-orbit continuation near the Hopf bifurcation point. Since the first Lyapunov coefficient is positive, the detected Hopf bifurcation is subcritical, which implies that the small-amplitude periodic branch emerging near the Hopf point is locally unstable. Furthermore, continuation from the Hopf point detects a limit point of cycles (LPC), indicating that the periodic-orbit branch undergoes a fold and experiences a change in stability along the branch. Biologically, this result shows that the system enters a sensitive oscillatory regime near the threshold value, where small parameter changes may alter the qualitative behavior of harvesting effort and fish density.

These findings are qualitatively related to the results of Ibrahim [16], where a critical biomass threshold also plays an important role in determining harvesting dynamics. In that study, the emphasis was placed on optimal harvesting and marine reserve management, whereas the present work focuses on local stability and bifurcation structure in a mangrove detritus–small fish system. Our results extend this perspective by showing that, in addition to regulating the persistence of harvesting effort, the threshold parameter may also induce changes in equilibrium stability and oscillatory dynamics through bifurcation mechanisms.

Overall, Figures 3 and 4 show that the threshold parameter a plays a central role in shaping the long-term harvesting dynamics. The bifurcation diagram reveals stability changes and the presence of multiple equilibrium branches, while periodic-orbit continuation near the Hopf point shows that the oscillatory regime is structurally sensitive. In particular, the subcritical Hopf bifurcation and the detected limit point of cycles indicate that small changes in the threshold may alter both equilibrium stability and periodic behavior. These results highlight the threshold parameter as a key mechanism governing qualitative transitions in the mangrove detritus–small fish system with adaptive harvesting effort.

4. Conclusion

This study developed and analyzed a three-dimensional mangrove detritus–small fish model with dynamic harvesting effort under a Beddington–DeAngelis functional response. The analysis showed that the model admits biologically feasible equilibrium states, including a coexistence equilibrium with positive harvesting effort and a coexistence equilibrium without harvesting effort under certain parameter conditions. Local stability analysis confirmed the conditions under which these equilibria are stable.

Numerical simulations supported the analytical results by showing convergence to the stable active-harvesting equilibrium under the baseline parameter set, while a modified scenario with reduced detritus carrying capacity and increased fish mortality led the system to a no-effort equilibrium. In addition, bifurcation analysis with respect to the threshold parameter a revealed branch points, a limit point, and a subcritical Hopf bifurcation. Periodic-orbit continuation near the Hopf point further indicated a sensitive oscillatory regime and a change in stability along the periodic branch through the detection of a limit point of cycles.

Overall, the results highlight the threshold parameter as a key factor governing harvesting persistence, equilibrium stability, and qualitative transitions in the model dynamics. Because the parameter values used in this study are illustrative and not calibrated from empirical data, these findings should be interpreted as qualitative theoretical insights rather than direct management prescriptions. Future work may include empirical parameter estimation, seasonal forcing, stochastic disturbances, and a more detailed analysis of periodic-orbit stability in mangrove-related harvesting systems.

CRediT Authorship Contribution Statement

Donna Kurniasih: Conceptualization, Methodology, Formal Analysis, Investigation, Software (Maple/MATCONT/MATLAB), Writing Original Draft, Visualization. **Dian Savitri:** Conceptualization, Methodology, Supervision, Validation, Writing Review & Editing.

Declaration of Generative AI and AI-assisted technologies

Generative AI tools (including ChatGPT) were used in a limited manner to assist with language refinement, grammar editing, and improving clarity of presentation. All mathematical modeling, analytical derivations, numerical computations, simulation outputs, interpretation of results, and scientific conclusions were developed and verified by the authors. No generative AI tool was used to generate or validate the core scientific results.

Declaration of Competing Interest

The authors declare no competing interests.

Funding and Acknowledgments

The authors would like to thank the Department of Mathematics, FMNS, Surabaya State University, for providing facilities in the Modeling and Simulation Laboratory during the research. We would also like to express our gratitude to the Indonesian Ministry of Education, Science, and Technology, along with our research advisor, under the "Regular Fundamental Research" program under contract number B/74003/UN38.III.1/LK.04.00/2025.

Data Availability

This study does not use field or experimental datasets. The numerical values of parameters are used as illustrative case-study settings to demonstrate the qualitative dynamics of the proposed model. Simulation codes and generated figures are available from the corresponding author upon reasonable request.

References

[1] Laura Carugati, Beatrice Gatto, Eugenio Rastelli, Marco Lo Martire, Caterina Coral, Silvestro Greco, and Roberto Danovaro. "Impact of mangrove forests degradation on biodiversity and ecosystem functioning". In: *Scientific Reports* 8.1 (2018), p. 13298. DOI: 10.1038/S41598-018-31683-0.

[2] Selviani Selviani, Neviaty Putri Zamani, N. M. N. Natih, and Nurhayati Br Tarigan. "Analysis of Mangrove Leaf Litter Decomposition Rate in Mangrove Ecosystem of Muara Pagatan, South Kalimantan". In: *Jurnal Kelautan Tropis* 27.1 (2024), pp. 103–112. DOI: 10.14710/jkt.v27i1.21913.

[3] Jurlia Apriliani Tonti Riska, Abdul Syukur, and Lalu Zulkifli. "Association between Mangrove Types and Some Mangrove Crab Species in West Lombok Sheet Mangrove Ecosystem". In: *JPPIPA (Jurnal Penelitian Pendidikan IPA)* 9.7 (2023), pp. 5610–5619. DOI: 10.29303/jppipa.v9i7.4781.

[4] José Amorim Reis-Filho, Euan S. Harvey, and Tommaso Giarrizzo. "Impacts of small-scale fisheries on mangrove fish assemblages". In: *ICES Journal of Marine Science* 76.1 (2019), pp. 153–164. DOI: 10.1093/icesjms/fsy110.

[5] Ummi Usrotus Saydatul Wakhidah, Kartika Nugraheni, and Winarni Winarni. "Analysis of Mangrove Forest Resource Depletion Models due to The Opening of Fish Pond Land with Time Delay". In: *Jurnal Ilmu Dasar* 23.1 (2022), p. 65. DOI: 10.19184/jid.v23i1.23889.

[6] Chandrima Talapatra. "Stochastic Dynamics of Dual-Prey–Predator Interactions under Harvesting Pressure: Insights from the California Current Ecosystem". In: *Earthline Journal of Mathematical Sciences* (2025), pp. 989–1020. DOI: 10.34198/ejms.15625.9891020.

[7] Yuxia Wang and Yifu Dong. "A Food Chain Model with a Protection Zone". In: *Journal of Partial Differential Equations* 38.3 (2025), pp. 352–375. DOI: 10.4208/jpde.v38.n3.7.

[8] Md Golam Mortuja, Mithilesh Kumar Chaube, and Santosh Kumar. "Mathematical Study on a Dynamical Predator–Prey Model with Constant Prey Harvesting and Proportional Harvesting in Predator". In: *Discontinuity, Nonlinearity, and Complexity* 13.1 (2024), pp. 269–278. DOI: 10.5890/dnc.2024.06.005.

[9] Yuan Tian, Yang Liu, and Kaibiao Sun. "Complex dynamics of a predator–prey fishery model: The impact of the Allee effect and bilateral intervention". In: *Electronic Research Archive* 32.11 (2024), pp. 6379–6404. DOI: 10.3934/era.2024297.

[10] Yinghai Shao, Hengguo Yu, C. Jin, Jun-Kai Fang, and Min Zhao. "Dynamics analysis of a predator–prey model with Allee effect and harvesting effort". In: *Electronic Research Archive* 32.10 (2024), pp. 5682–5716. DOI: 10.3934/era.2024263.

[11] Yingying Wang and Zhinan Xia. "Periodic dynamics of predator–prey system with Beddington–DeAngelis functional response and discontinuous harvesting". In: *Boundary Value Problems* 2023 (2023), pp. 1–19. DOI: 10.1186/s13661-023-01806-2.

[12] Hanyan Liu and Jingli Xie. "Stability of a predator–prey model with Beddington–DeAngelis functional response and disease in the prey". In: *Applied Mathematical Sciences* 15.4 (2021), pp. 165–175. DOI: 10.12988/AMS.2021.914477.

[13] Wenchang Chen. "Stability and Bifurcation Analysis of a Predator–Prey Model with Michaelis–Menten Type Prey Harvesting". In: *Journal of Applied Mathematics and Physics* 10.2 (2022), pp. 504–526. DOI: 10.4236/jamp.2022.102038.

[14] Qiannan Song, Ruizhi Yang, Chunrui Zhang, and Lei Wang. "Bifurcation analysis of a diffusive predator–prey model with Beddington–DeAngelis functional response". In: *Journal of Applied Analysis and Computation* 11.2 (2021), pp. 920–936. DOI: 10.11948/20200119.

[15] Bushra E. Kashem and Hassan Fadhil Al-Husseiny. "The Dynamic of Two Prey–One Predator Food Web Model with Fear and Harvesting". In: *Partial Differential Equations in Applied Mathematics* 11 (2024), p. 100875. DOI: 10.1016/j.padiff.2024.100875.

[16] Mahmud Ibrahim. "Optimal harvesting of a predator–prey system with marine reserve". In: *Scientific African* 14 (2021), e01048. DOI: 10.1016/j.sciaf.2021.e01048.

[17] Daniel Zambelongo. "Optimal harvesting strategy for prey–predator model with fishing effort as a time variable". In: *Advances in Differential Equations and Control Processes* 31.3 (2024), pp. 417–438. DOI: 10.17654/0974324324023.

[18] Gleb Polevoy, Stojan Trajanovski, and Mathijs de Weerdt. "When Effort May Fail: Equilibria of Shared Effort with a Threshold". In: *Social Science Research Network* (2022), p. 53. DOI: 10.2139/ssrn.4179253.

[19] Prisalo Luis, Putri Zahra Kamalia, Olumuyiwa James Peter, and Dipo Aldila. "Implementation of non-standard finite difference on a predator prey model considering cannibalism on predator and harvesting on prey". In: *Jambura Journal of Biomathematics* 6.1 (2025), pp. 35–43. DOI: 10.37905/jjbm.v6i1.30550.

[20] Dian Savitri, A. Sofro, and Dimas Avian Maulana. "Hopf Bifurcation for Detritus Food Chain in Mangrove Ecosystem". In: *MATEC Web of Conferences* 372 (2022), p. 05007. DOI: 10.1051/matecconf/202237205007.

[21] Koushik Garain and Partha Sarathi Mandal. "Bifurcation Analysis of a Prey–Predator Model with Beddington–DeAngelis Type Functional Response and Allee Effect in Prey". In: *International Journal of Bifurcation and Chaos* 30.16 (2020), p. 2050238. DOI: 10.1142/S0218127420502387.